

A Local Mesh Refinement Algorithm for the FDFD Method Using a Polygonal Grid

H. Klingbeil, K. Beilenhoff, and H. L. Hartnagel

Abstract—A local mesh refinement algorithm for the finite-difference method in the frequency domain (FDFD) is presented that is based on polygonal grids. It is applied to a simple test structure for which the propagation parameters were computed with a mode-matching method as a reference. It is shown that the local mesh refinement realized with this polygonal grid significantly improves the accuracy of the propagation constant compared to the conventional FD method based on rectangular meshes.

I. INTRODUCTION

USUALLY, the finite-difference method in the frequency domain (FDFD) is used with a nonequidistant cartesian grid (Yee's grid) [1]–[3]. The electrical field components are defined on the mesh lines whereas the magnetic components are located on a dual grid. In order to allow a better approximation of curvilinear geometries, tetrahedral cells can also be proposed as an alternative. However, to ensure the orthogonality between the grid and the dual grid, one faces the problem that the field components of the dual grid can be defined outside the surface of the cell they belong to. This problem arises especially if an angle between meshlines is greater or equal 90°. Due to this restriction it is extremely difficult to implement an automatic mesh-generation for FD field theoretical methods. However, for many applications the standard nonequidistant cartesian grid is still sufficient, and with a local mesh refinement extension a better approximation of arbitrarily shaped structures can be obtained with lower numerical effort.

Until now, such local mesh refinement algorithms were only presented in connection with time domain methods [4]–[6]. The interpolation of the field components used at the interface between the two meshes leads to various problems if it is transferred to the frequency domain case. For instance, high errors were found when this kind of local mesh refinement was applied to coplanar waveguides.

In this letter, a local mesh refinement will be presented for the two-dimensional (2-D) case, which, therefore, uses a polygonal orthogonal grid at the interface. Although the algorithm was developed for arbitrary polygons, only triangles and rectangles are needed in this case.

The method can be extended to three-dimensional (3-D) problems.

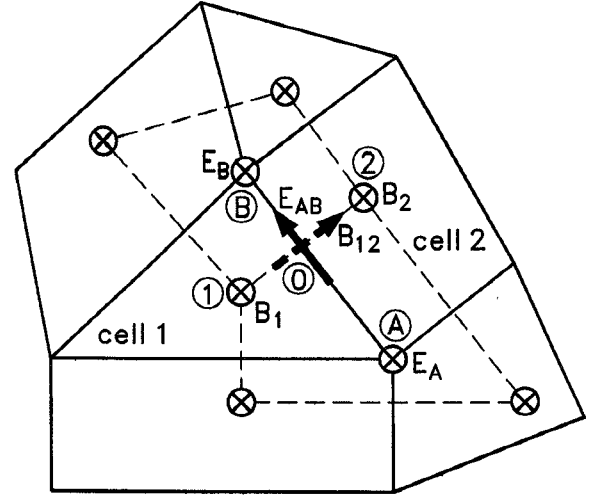


Fig. 1. Polygonal grid.

II. THE NUMERICAL METHOD

In the following the FD method for polygonal grids is described in detail. Then the transition cell that forms the interface between the two meshes and which consists of a simple polygonal grid is presented.

A. Polygonal Grid

Fig. 1 shows a section of a 2-D polygonal grid. The transversal electric field components are located on the polygon lines (in the figure only one component E_{AB} is shown). The longitudinal electric field components are defined at the mesh points of the polygons (two of the mesh points in the figure are marked with A and B, the corresponding field components are E_A and E_B). The transversal magnetic field components are defined on the grid-lines of the dual mesh and, therefore, are perpendicular to the transversal electric field components (one component B_{12} is shown in the figure). The longitudinal magnetic field components (e.g. B_1 and B_2) are located at the mesh points of the dual grid.

In the following the vector \vec{s}_{XY} is a vector that points from X to Y.

By substituting $\vec{B}' = -j\omega\vec{B}$, where \vec{B} denotes the magnetic flux density, and assuming a time harmonic dependence ($f(t) = e^{j\omega t}$) Maxwell's equations in integral form can be written as follows:

$$k_0^2 \int_A \epsilon_r \vec{E} \cdot d\vec{A} = \oint_{\partial A} \frac{\vec{B}'}{\mu_r} \cdot d\vec{s} \quad (1)$$

Manuscript received August 18, 1995.

The authors are with the Institut für Hochfrequenztechnik, Technische Hochschule Darmstadt, 64283 Darmstadt, Germany.

Publisher Item Identifier S 1051-8207(96)00454-0.

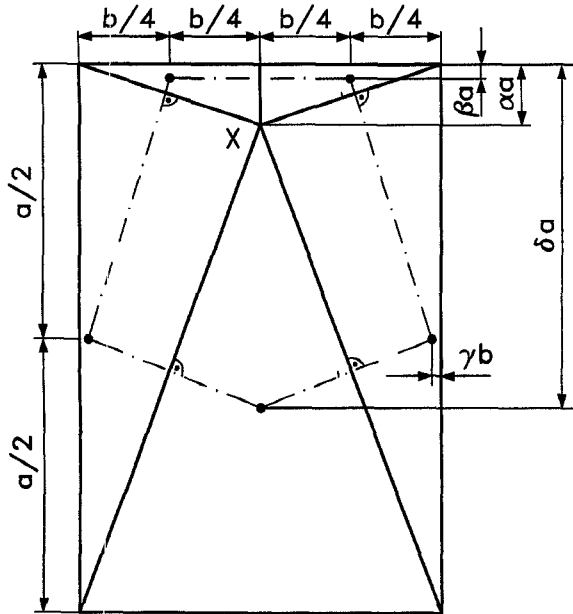


Fig. 2. Transition cell.

$$\int_A \vec{B}' d\vec{A} = \oint_{\partial A} \vec{E} d\vec{s}. \quad (2)$$

If these equations are transferred into the Finite-Difference scheme [3] and the $e^{-jk_z z}$ -dependency of the fields is taken into account, one obtains

$$\begin{aligned} & \left(k_z^2 - \frac{F_{AB}^E F_{12}^B k_0^2}{G_{AB}^E G_{12}^B} \right) E_{AB} + \frac{1}{G_{AB}^E} (jk_z E_A - jk_z E_B) \\ & + \frac{F_{12}^B}{G_{12}^B G_{AB}^E} \left(\frac{B_2'}{\mu_2} - \frac{B_1'}{\mu_1} \right) = 0. \end{aligned} \quad (3)$$

In this equation, all variables F and G are scalar quantities. These are obtained if integrals are approximated by simple products. F corresponds to a surface integral whereas G corresponds to a contour integral. The upper index indicates if either the electric field or the magnetic field is integrated. The lower index denotes the orientation of the field component.

For example, F_{AB}^E is an integration factor with

$$F_{AB}^E E_{AB} \approx \int_{1-2} \epsilon_r \vec{E} d\vec{a}. \quad (4)$$

It has to be taken into account that the size of a cell in the longitudinal direction is infinitely thin, so that the surface integral in (4) degenerates to a simple contour-integral (note that $d\vec{a}$ is perpendicular to \vec{s}_{12}). Therefore, one finds

$$F_{AB}^E = \epsilon_1 |\vec{s}_{10}| + \epsilon_2 |\vec{s}_{20}| \quad (5)$$

ϵ_1 and ϵ_2 are the relative complex permittivities of elementary cells 1 and 2, respectively.

The other factors can be found similarly by

$$F_{12}^B B_{12}' \approx \int_{B-A} \vec{B}' d\vec{a},$$

$$G_{AB}^E E_{AB} \approx \int_{A-B} \vec{E} d\vec{s},$$

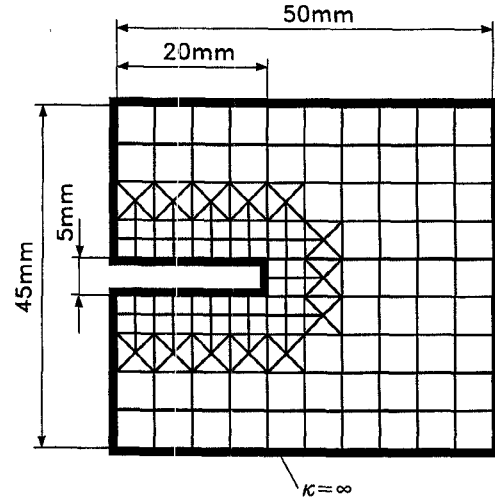


Fig. 3. Test structure discretized with a local mesh refinement.

$$G_{12}^B B_{12}' \approx \int_{1-2} \frac{\vec{B}'}{\mu_r} d\vec{s} \quad (6)$$

$jk_z E_A$ or $jk_z E_B$ can be substituted in (3) by using the divergence condition $\oint \epsilon_r \vec{E} d\vec{A} = 0$. One finds

$$jk_z E_A = \frac{1}{F_A^E} \sum_i F_i^E E_i, \quad F_A^E E_A \approx \int \epsilon_r \vec{E} d\vec{A}.$$

The summation has to be performed over all transversal electric field components E_i , which are defined on grid lines beginning at corner A (E_{AB} also belongs to this set).

The field components B_1 and B_2 in (3) can also be substituted by using a discretized form of (2)

$$B_1' = \frac{1}{F_1^B} \sum_i G_i^E E_i, \quad F_1^B B_1' \approx \int \vec{B}' d\vec{A}.$$

In this sum, all transversal electric field components E_i have to be considered which surround point 1 clockwise.

After all substitutions there is one equation for each E_i which is described by the other electric field components and the square of the propagation constant k_z . Due to the linear dependance between the unknowns a complex algebraic eigenvalue problem $(\mathbf{A} - \lambda \mathbf{I}) \mathbf{x} = \mathbf{0}$ is obtained where $\lambda = -k_z^2$. The transversal electric field distribution corresponds to \mathbf{x}_2 .

B. Transition Cell

For the interface between coarse grid and fine grid, a cell as shown in Fig. 2 is applied. It is not possible to achieve orthogonality between the electric and magnetic field components if mesh point X is located in the middle of the cell. Thus, this point has to be shifted to form an orthogonal grid. The positions of the mesh points are defined as follows:

$$\alpha = \frac{1}{4} \frac{b^2}{a^2}, \quad \beta = \frac{\alpha}{4}, \quad \gamma = \frac{\alpha}{8}, \quad \delta = \frac{\alpha^2/2 - \alpha - 1}{2(\alpha - 1)}. \quad (7)$$

The following restriction has to be taken into account: the parameters given in (7) should be used only for $\frac{b}{a} \leq 1$. Usually, the grid can be chosen accordingly. For different

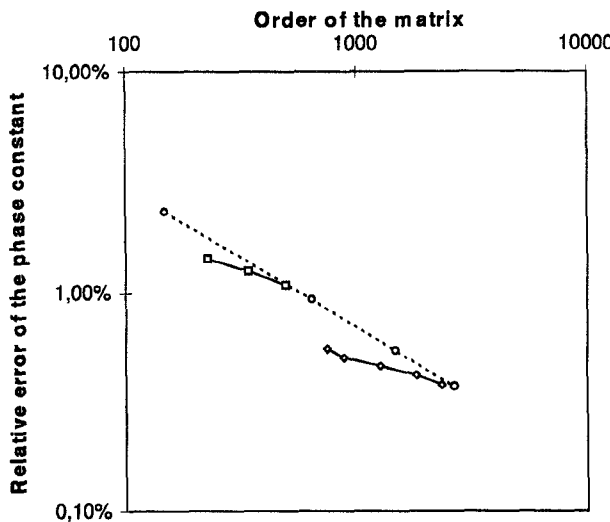


Fig. 4. Error of the propagation constant for the test structure at $k_0 = 70 \text{ m}^{-1}$ conventional method (Yee's grid); — local mesh refinement; \diamond coarse cell size $ds = 2.5 \text{ mm}$; \square coarse cell size $ds = 5 \text{ mm}$.

values of $\frac{b}{a}$, the mesh points of the dual grid calculated by (7) will be too close to the original grid lines. It is possible to determine a second set of parameters α, β, γ and δ which holds for $1 < \frac{b}{a} < 2$. For $\frac{b}{a} > 2$, however, no solution exists.

III. NUMERICAL RESULTS

Fig. 3 shows the test structure analysed with the proposed method. It is a simple rectangular waveguide with a conducting slab. This structure was chosen since a local mesh refinement according to Fig. 3 is useful to obtain a high field resolution at the edge. The simple geometry also enables one to determine the propagation constant with a very high accuracy by means of a mode-matching method. For $k_0 = 70 \text{ m}^{-1}$ one finds $k_z = 52.42 \text{ m}^{-1}$ with an extrapolated error below 0.01%.

In Fig. 4 the error of the propagation constant is presented against the matrix order. The dotted curve is obtained with an equidistant discretization of the structure. For the two other curves a local mesh refinement as shown in Fig. 3 was applied. The location of the interface between the two grids varies, i.e. the area of the local mesh is increased, which also leads to

higher orders of the matrix. The curves constructed by this scheme end at the dotted curve since increasing the size of the local mesh will finally result in a structure with a fine mesh everywhere.

One can observe that all results obtained with a local mesh refinement provide smaller errors. Computations carried out for a coplanar waveguide also show improved results for both the phase and the attenuation constant.

IV. CONCLUSION

A new local mesh refinement algorithm for the finite-difference method in the frequency domain was presented. It is based on a noncartesian polygonal grid at the interface. The method was applied to a test structure for which a highly reliable reference calculation was performed. It could be shown that the accuracy of the propagation constant computed with the new method is significantly higher than that calculated with a conventional method using a cartesian grid. The method of polygonal grids is not restricted to local mesh refinements. It can also be applied for arbitrarily shaped (e.g. round) structures in order to allow a better approximation.

REFERENCES

- [1] T. Weiland, "Three dimensional resonator mode computation by finite difference method," *IEEE Trans. Magn.*, vol. MAG-21, no. 6, pp. 2340-2343, Nov. 1985.
- [2] A. Christ and H. L. Hartnagel, "Three-dimensional finite-difference method for the analysis of microwave-device embedding," *IEEE Trans. Microwave Theory Tech.*, vol. 35, no. 8, pp. 688-696, Aug. 1987.
- [3] K. Beilenhoff, W. Heinrich, and H. L. Hartnagel, "Improved finite-difference formulation in frequency domain for three-dimensional scattering problems," *IEEE Trans. Microwave Theory Tech.*, vol. 40, no. 3, pp. 540-546, Mar. 1992.
- [4] M. Rittweger, "Simulation transienter elektrodynamischer ausbreitungsphänomene zur analyse der übertragungseigenschaften von systemen der mikro-und millimeterwellentechnik," dissertation, Universität Duisburg, Germany, 1992.
- [5] S. S. Zivanovic, K. S. Yee, and K. K. Mei, "A subgridding method for the time-domain finite-difference method to solve Maxwell's equations," *IEEE Trans. Microwave Theory Tech.*, vol. 39, no. 3, pp. 471-479, Mar. 1991.
- [6] I. S. Kim and W. J. R. Hoefer, "A local mesh refinement algorithm for the time domain-finite difference method using Maxwell's Curl equations," *IEEE Trans. Microwave Theory Tech.*, vol. 38, no. 6, pp. 812-815, June 1990.